

# SPIN PHYSICS AT $e^+e^-$ COLLIDERS

WALTER BONIVENTO

*Laboratoire de l'Accélérateur Linéaire  
IN2P3-CNRS et Université de Paris-Sud  
BP34, F-91898 Orsay, France*

A large number of measurements with polarized beams and/or spin analysis of final state particles has been performed at the  $e^+e^-$  colliders LEP and SLC, providing important information on the dynamics of high energy interactions. In this paper three subjects, for which the role of spin studies was particularly relevant, will be covered: the measurements of the electroweak couplings, the study of fragmentation dynamics and the search for physics beyond the Standard Model.

## 1. Electroweak physics

The measurement of the electroweak couplings of the Z to the fermions has been one of the main goals of the high energy colliders LEP (during the first six years of running) and SLC. Spin effects provide sensitive measurements of the electroweak couplings and allow to perform accurate tests of the Standard Model.

From the experimental point of view, high energy  $e^+e^-$  colliders allow to select the different final states with high efficiency and low background.

### 1.1. The $e^+e^-$ reaction at LEP1

The differential cross-section for fermion-antifermion production,  $e^+e^- \rightarrow f\bar{f}$ , in the Standard Model (or more generally in a model with chirality-conserving interactions) can be written, at tree level, around the Z resonance and for unpolarized  $e^\pm$  beams, as [1,2]:

$$\frac{d\sigma}{d\Omega} = \frac{1}{4\pi^2 q^2} |P(q^2)|^2 (A + B_{1\mu} s_{f+}^\mu + B_{2\mu} s_{f-}^\mu + C_{\mu\nu} s_{f+}^\mu s_{f-}^\nu) \quad (1)$$

where  $P(q^2)$  is the Z propagator,  $s_{f+}^\mu$  and  $s_{f-}^\mu$  the covariant spin vectors of the outgoing fermions. Only the Z exchange contribution is included, being dominant over the other ones.

The spin-independent term is

$$A = C_0(1 + \cos^2\theta) + 2C_1 \cos\theta \quad (2)$$

with  $C_0 = (|v_e|^2 + |a_e|^2)(|v_f|^2 + |a_f|^2)$  and  $C_1 = 4\text{Re}(v_e a_e^*)\text{Re}(v_f a_f^*)$  where  $\theta$  is the outgoing fermion  $f$  polar angle with respect to the  $e^-$  direction,  $v_f$  and  $a_f$ ,  $f = e, \mu, \tau$ , are the electroweak vector and axial coupling constants (for simplicity radiative corrections will be neglected in the following). The second term of Eq.(2) gives rise to a forward-backward asymmetry of the cross-section.

Using the coordinate system in the laboratory frame where the  $z$  axis is along the outgoing fermion  $f$  direction and the  $y$  axis is normal to the reaction plane, at leading order in  $m_f$ :

$$B_{1\mu} s_{f+}^\mu + B_{2\mu} s_{f-}^\mu = -D_0(s_{f+}^{*z} + s_{f-}^{*z})(1 + \cos^2\theta) - D_1(s_{f+}^{*z} + s_{f-}^{*z})2\cos\theta \quad (3)$$

where  $s_{f\pm}^*$  designates the polarization vector in the  $f^\pm$  rest frame.

The two terms of Eq.(3) give rise to the mean longitudinal final-state polarization asymmetry (a parity(P)-odd observable)

$$\langle P_f \rangle = -\frac{D_0}{C_0} = -2\frac{\text{Re}(v_f a_f^*)}{|v_f|^2 + |a_f|^2} \equiv -\mathcal{A}_f \quad (4)$$

and to the forward-backward polarization asymmetry (P-odd)

$$A_{pol}^{FB} = -\frac{3}{4} \frac{D_1}{C_0} = -\frac{3}{4} \cdot \frac{Re(v_e a_e^*)}{|v_e|^2 + |a_e|^2} = -\frac{3}{4} \mathcal{A}_e \quad (5)$$

The latter observable is also related to the  $Z$  polarization as  $P_Z = -\mathcal{A}_e$ . Other terms related to transverse spin components are suppressed by  $m_f/M_Z$ . Using the notation of Eqs.(4,5), the spin-independent term of Eq.(1) can be rewritten as

$$A \propto (1 + \cos^2\theta) - 2\mathcal{A}_f P_Z \cos\theta \quad (6)$$

The quadratic term in the spin of Eq.(1) gives rise to the spin correlations:

$$C_{\mu\nu} s_{f+}^\mu s_{f-}^\nu = C_0 h_0 + C_1 h_1 + C_2 h_2 + D_2 h_3 \quad (7)$$

with

$$h_0 = s_{f+}^{*z} s_{f-}^{*z} (1 + \cos^2\theta) \quad (8)$$

$$h_1 = s_{f+}^{*z} s_{f-}^{*z} 2\cos\theta \quad (9)$$

$$h_2 = (s_{f+}^{*y} s_{f-}^{*y} - s_{f+}^{*x} s_{f-}^{*x}) \sin^2\theta \quad (10)$$

$$h_3 = (s_{f+}^{*y} s_{f-}^{*x} + s_{f+}^{*x} s_{f-}^{*y}) \sin^2\theta \quad (11)$$

The terms  $h_0$  and  $h_1$  represent the longitudinal spin correlation,  $h_2$  the transverse-transverse spin correlation, whose coefficient is  $C_{TT} \equiv C_2/C_0 = (|a_f|^2 - |v_f|^2)/(|a_f|^2 + |v_f|^2)$  and  $h_3$  the transverse-normal spin correlation, with coefficient  $C_{TN}$  (P-odd and T-odd). In the Standard Model, at tree level, the values of the  $Z$  couplings to fermions depend on one parameter, the Weinberg angle  $\theta_W$ . For  $\sin^2\theta_W = 0.232$ ,  $\mathcal{A}_l = 0.15$ ,  $\mathcal{A}_u = 0.67$  and  $\mathcal{A}_d = 0.935$ . The longitudinal spin correlation is one by helicity conservation and, for leptonic final states,  $C_{TT} = 0.99$  and  $C_{TN} = -0.01$  [3].

## 1.2. The $\tau$ decay as polarization analyser

The  $\tau$  spin vectors are not directly observable. The  $\tau$  weak decay products can be used as  $\tau$  spin analyser. In the  $\tau^\pm$  rest frame

$$d\Gamma_X^\pm(\mathbf{s}_{\tau^\pm}^*) \propto \left( 1 \pm \alpha_X m_\tau \frac{(\mathbf{q}_{\tau^\pm}^* \cdot \mathbf{s}_{\tau^\pm}^*)}{(\mathbf{q}_i^* \cdot \mathbf{p}_{\tau^\pm})} \right) d\Omega_{\tau^\pm}^* \quad (12)$$

where  $\mathbf{q}_{\tau^\pm}^*$  is the momentum of the  $\tau^\pm$  decay product,  $\mathbf{p}_{\tau^\pm}$  is the momentum of the  $\tau^\pm$  in the laboratory frame,  $\Gamma_X^\pm$  is the  $\tau^\pm$  partial decay width in the decay channel  $X$ .  $\alpha_X$  is a constant whose value depends on the decay channel  $X$  and is called *analysing power*. By CP invariance  $P_{\tau^+} = -P_{\tau^-}$ ; from Eq.(12) it is seen that particle and anti-particles have the same decay spectra. By definition it will be taken  $P_\tau \equiv P_{\tau^-}$ .

## 1.3. Measurement of the $\tau$ longitudinal polarization

The  $\tau$  polarization was measured from the study of single  $\tau$  decay products spectra. A method based on the acollinearity spectrum of the  $\tau$  decay products was also used, though it was found to be less sensitive to the polarization. It was also shown [4,5] that, when both  $\tau$ 's decay semileptonically, an optimal sensitivity can be obtained by reconstructing the  $\tau$  direction. For what concerns their decay spectra, semileptonic and leptonic decays have to be treated in a different way.

### 1.3.1. Spin-0 hadronic system ( $\tau \rightarrow \pi(K)\nu_\tau$ )

There are two amplitudes for the decay, corresponding to the two possible  $\tau$  polarization states:  $A^+ \propto \cos\theta^*/2$  and  $A^- \propto \sin\theta^*/2$ , where  $\theta^*$  is the angle in the  $\tau$  rest frame of the hadron momentum

with respect to the polarization axis of the  $\tau$  (defined as its direction of motion in the laboratory frame). Then:

$$W(\cos\theta^*) = \frac{dN}{d\cos\theta^*} \propto \frac{1+P_\tau}{2}|A^+|^2 + \frac{1-P_\tau}{2}|A^-|^2 = [1 + P_\tau \cos\theta^*] \quad (13)$$

The analysing power, defined as in Eq.(12), for this decay is  $\alpha_\pi = -1$ . In the two body decay of the  $\tau$  the angle  $\theta^*$  is fully correlated to the hadron energy in the lab frame:  $\cos\theta^* \simeq 2x_\pi - 1$  with  $x_\pi = (E_\pi/E_{beam})_{LAB}$ . Therefore more energetic hadrons correspond to  $P_\tau = +1$ .

### 1.3.2. Spin-1 hadronic system ( $\tau \rightarrow \rho(K^*)\nu_\tau$ , $\tau \rightarrow a_1\nu_\tau$ )

In this case there are four decay amplitudes, for the two allowed hadronic system helicities  $\lambda_X = 0, -1$ ,  $X = \rho, a_1$  and  $W(\cos\theta^*) \propto 1 + P_\tau \alpha_X \cos\theta^*$ , with  $\alpha_X = (m_\tau^2 - 2m_X^2)/(m_\tau^2 + 2m_X^2)$ . With respect to the pion decay, the analysing power is reduced:  $\alpha_\rho = -0.46$  for  $\tau^- \rightarrow \rho^- \nu_\tau$  and  $\alpha_{a_1} = -0.12$  for  $\tau^- \rightarrow a_1^- \nu_\tau$ .

To regain sensitivity it is possible to measure the hadron spin composition from the spectra of its decay products. For the decay  $\tau^- \rightarrow \rho^- \nu_\tau$ , in the  $\rho$  frame,  $dN(\rho_T \rightarrow \pi\pi)/d\cos\psi^* \propto \sin^2\psi^*$  and  $dN(\rho_L \rightarrow \pi\pi)/d\cos\psi^* \propto \cos^2\psi^*$ , where  $\rho_T$  and  $\rho_L$  indicate a transversely and longitudinally polarized  $\rho$ , respectively, and  $\psi^*$  is the angle, in the  $\rho$  frame, of the charged  $\pi$  with respect to the polarization axis of the  $\rho$ . Like  $\theta^*$ ,  $\psi^*$  can also be reconstructed from measured particle energies in the lab system as  $\cos\psi^* = (2x_\rho - 1)\sqrt{1 - 4m_\pi^2/m_\rho^2}$  with  $x_\rho = (E_\pi/E_\rho)_{LAB}$ . Most of the information on the  $\tau$  polarization is therefore contained in the two-dimensional distribution  $W(\theta^*, \psi^*)$ .

An optimal one-dimensional variable,  $\omega$ , with maximal sensitivity to the  $\tau$  polarization was derived in [4]. Indeed, given  $W(\vec{x}) \propto f(\vec{x}) + P_\tau g(\vec{x})$ , where  $\vec{x}$  is the vector whose components are the variables which the distribution depends on, the optimal variable is  $\omega = g(\vec{x})/f(\vec{x})$ .

For the decay  $\tau^- \rightarrow a_1^- \nu_\tau$ ,  $a_1 \rightarrow 3\pi$  similar arguments apply, though there is a residual  $a_1$  decay model dependence which cannot be factorized out and remains as a systematic uncertainty on  $P_\tau$  [6].

### 1.3.3. Leptonic decays

In the  $\tau$  frame  $dN/(dx_l^* d\cos\theta^*) \propto x_l^{*2}[(3 - 2x_l^*) + P_\tau(1 - 2x_l^*)\cos\theta^*]$ , where  $x_l^* = 2E_l^*/m_\tau$  and  $E_l^*$  is the charged lepton energy. For leptonic decays  $\alpha_l = 1/3$ , of opposite sign with respect to hadronic decays. In the laboratory system, contrary to the hadronic case,  $P_\tau = -1$  gives more energetic leptons.

The sensitivity to the longitudinal polarization for a given  $\tau$  decay channel  $X$  is defined as  $S_X \equiv 1/(\Delta P_\tau^X \sqrt{N})$ , where  $N$  is the number of selected events used to obtain an error  $\Delta P_\tau^X$  on the polarization. Table 1 lists the different sensitivities for the various  $\tau$  decay channels, in the case of an ideal detector.

decay channel $X$	$S_X$	$B_X$	$w_X$
$\tau^- \rightarrow \pi^- \nu_\tau$	0.58	0.12	1
$\tau^- \rightarrow \rho^- \nu_\tau$	0.49 (0.58*)	0.26	1.6
$\tau^- \rightarrow a_1^- \nu_\tau$	0.45 (0.58*)	0.10	0.5
$\tau^- \rightarrow e^- \bar{\nu}_e \nu_\tau$	0.22	0.18	0.2
$\tau^- \rightarrow \mu^- \bar{\nu}_\mu \nu_\tau$	0.22	0.17	0.2

Table 1

Sensitivity  $S_X$  for an ideal detector to the  $\tau$  polarization for the decay channel  $X$  [4], branching ratio  $B_X$  and relative weight  $w_X = S_X^2 B_X$  in the average of the results of the different decay channels [7], normalised to the pion value (\* = using the reconstruction of the  $\tau$  direction [5]).

The measurement of  $P_\tau$  as a function of  $\theta$  allows to extract at the same time  $\mathcal{A}_\tau$  and  $P_Z$ :

$$P_\tau(\cos\theta, P_e) = -\frac{(1 + \cos^2\theta)\mathcal{A}_\tau - 2\cos\theta P_Z}{(1 + \cos^2\theta) - 2\cos\theta\mathcal{A}_\tau P_Z} \quad (14)$$

#### 1.4. Measurement of the $\tau^+\tau^-$ transverse spin correlations

Introducing the  $\tau$  decay in Eq.(1) one obtains:

$$\frac{d\sigma(X_+, X_-)}{d\epsilon d\cos\theta_- d\phi} = \frac{|P(q^2)|^2}{4q^2} (F_0(\epsilon)(1 + \cos^2\theta_-) + F_1(\epsilon)2\cos\theta_- + F_2(\epsilon, \phi)\sin^2\theta_-) \quad (15)$$

where

$$\begin{aligned} F_n(\epsilon) &= C_n[Q_1(\epsilon) + \alpha_{X_+} \cdot \alpha_{X_-} Q_2(\epsilon)] + D_n(\alpha_{X_+} - \alpha_{X_-})Q_3(\epsilon) \\ F_2(\epsilon, \phi) &= \alpha_{X_+} \cdot \alpha_{X_-} [C_2\cos 2\phi + D_2\sin 2\phi]Q_4(\epsilon) \end{aligned} \quad (16)$$

with  $n = 0, 1$ ,  $\theta_-$  the polar angle of  $\tau^-$  decay product,  $X_+$  and  $X_-$  the  $\tau^+$  and  $\tau^-$  decay channel, respectively,  $\epsilon$  the acollinearity angle between the two  $\tau$  decay products and  $\phi$  the aplanarity angle, defined as the azimuthal angle of the  $e^-$  beam axis in a reference frame where the z axis is along the momentum of  $\tau^-$  decay product and the momentum of  $\tau^+$  decay product is contained in the  $x - z$  plane. The complete expression of the  $Q_i(\epsilon)$ ,  $i = 1, 4$ , functions can be found in [2].

The transverse spin correlations are given by the terms  $C_2, D_2$  in Eq.(16). They are therefore expected to be observed as  $\phi$  modulation of the cross-section, with an amplitude depending on the product  $\alpha_{X_+}\alpha_{X_-}$ . Therefore opposite signs are expected for hadron-hadron and hadron-lepton events, respectively. This was indeed observed [8,3], as shown in figure 1. One experiment [3] obtained  $C_{TT} = 1.06 \pm 0.14$  and  $C_{TN} = 0.08 \pm 0.14$ , in agreement with the Standard Model predictions.

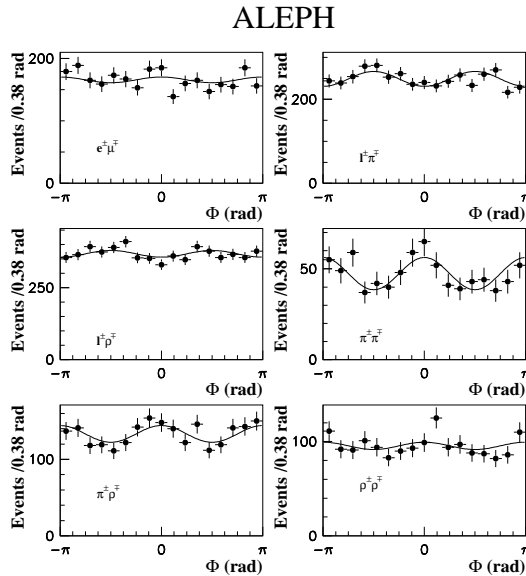


Fig. 1. Transverse spin correlations: aplanarity angle, as defined in the text, distributions. The curve shows the Standard Model prediction normalised to the total number of events [3].

### 1.5. The $\tau^+\tau^-$ longitudinal spin correlations

Assuming helicity conservation in high energy  $e^+e^-$  interactions, the measurement of the longitudinal spin correlations can be interpreted as a measurement of the  $\nu_\tau$  helicity ( $h_{\nu_\tau}$ ). Experiments without beam polarization measured the absolute value of  $h_{\nu_\tau}$  using this correlation [9,10] and both the absolute value and the sign from  $\tau^- \rightarrow a_1^- \nu_\tau$  decay spectra, though with modest precision [11].

At SLC a highly longitudinally polarized electron beam,  $|P_{e^-}| > 75\%$ , collides with an unpolarized positron beam, giving rise to highly longitudinally polarized  $\tau$ 's. Indeed, Eq.(14) is still valid with

$$P_Z = -\frac{\mathcal{A}_e - P_e}{1 - \mathcal{A}_e P_e} \quad (17)$$

Therefore  $P_Z(P_{e^-} > 0) = 0.70$  and  $P_Z(P_{e^-} < 0) = -0.83$  while  $P_Z(P_{e^-} = 0) = -0.16$ . With appropriate combinations of beam polarization and angular regions in  $\theta$ , it is possible to measure  $\tau$  spectra which are sensitive to both the magnitude and the sign of the neutrino helicity as shown in figure 2. In [12]  $h_{\nu_\tau} = -0.94 \pm 0.09$  was obtained.

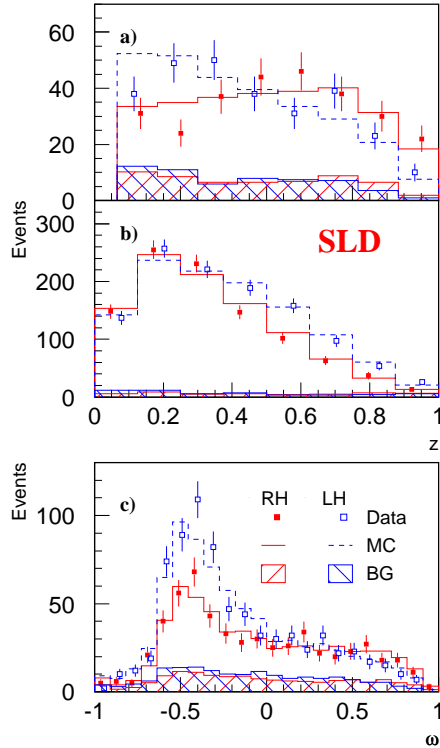


Fig. 2.  $\tau$  decay spectra for a)  $\tau^- \rightarrow \pi^- \nu_\tau$  and b)  $\tau^- \rightarrow l^- \bar{\nu}_l \nu_\tau$ , where  $z$  is the ratio of the charged  $\tau$  decay product energy to beam energy in the laboratory frame and for c)  $\tau^- \rightarrow \rho^- \nu_\tau$ , with  $\omega$  defined as in [4]. The dots and lines classified as L.H.(left-handed) correspond to the selection ( $\cos\theta > 0, P_e < 0$ ) and ( $\cos\theta < 0, P_e > 0$ ): the  $\tau^-$  is expected to be predominantly left-handed and therefore the  $\pi$  and  $\rho$  spectra are expected to be softer and the lepton spectrum is expected to be harder, as observed in the data. From [12].

### 1.6. Measurements of the Z couplings at SLC

At SLC, with beam polarization  $P_e^-$ , the spin-independent term of Eq.(1) has the same form of Eq.(6), though with  $P_Z$  defined as in Eq.(17). A larger forward-backward asymmetry than at LEP is then expected, resulting in a sensitivity higher by more than a factor 4 to the  $\mathcal{A}_f$  measurement. The possibility at SLC to invert the beam polarization allows to define an observable which is not accessible at LEP, the left-right asymmetry:

$$A_{LR} = \frac{\sigma_L - \sigma_R}{\sigma_L + \sigma_R} = \frac{1}{|P_e|} \cdot \frac{N_L - N_R}{N_L + N_R} = \mathcal{A}_e \quad (18)$$

where  $N_L$  ( $N_R$ ) is the number of selected events with negative (positive) polarization of the electron beam. Due to its linear dependence on  $\mathcal{A}_e$  and to the relatively high statistics that can be collected with an inclusive  $e^+e^- \rightarrow q\bar{q}$  selection, the left-right asymmetry gives a very precise measurement of  $\mathcal{A}_e$ .

### 1.7. Extraction of the Weinberg angle

In the context of the Standard Model, from the different measurements of  $\mathcal{A}_f$ , an estimate of the Weinberg angle was obtained.

As is shown in a recent review of the subject [13], the  $\tau$  polarization at LEP and the left-right asymmetry at SLC are among the most sensitive measurements of the Weinberg angle, to which they contribute with a relative error of 0.18% and 0.13%, respectively.

## 2. Fragmentation dynamics

At LEP/SLC energies final state quarks and gluons give rise to multi-particle jets in the detectors. Very often studies of spin effects are concentrated on the highest momentum, named leading, particle of these jets, under the hypothesis that the quark initiating the jet is carried by this particle and the quark quantum numbers are transferred to it. A prerequisite for spin studies is that the sign of the charge (taking into account the possible quark combinations in a hadron) and the flavour are transferred from the quark to the leading hadron.

In  $b\bar{b}$  and  $c\bar{c}$  events B and D hadrons are produced with hard fragmentation functions and at a rate of about two per event. It is therefore plausible that they carry the initial quark and its quantum numbers.

For light quark events a measurement was performed at SLC [14]. The electroweak theory predicts that the quark ( $q$ ) jet should mostly follow the  $e^-$  ( $e^+$ ) beam direction for  $P_e = -1(+1)$ . In this way quark-initiated jets can be selected with 73% purity. The asymmetry  $D_h = (N^+ - N^-)/(N^+ + N^-)$ , where  $N^+ = N(q \rightarrow h) + N(\bar{q} \rightarrow \bar{h})$ ,  $N^- = N(q \rightarrow \bar{h}) + N(\bar{q} \rightarrow h)$  and  $h$  is the leading hadron in the jet, was measured and found to be significantly different from zero for relatively large momentum fractions of the leading proton,  $\Lambda$ ,  $K^\pm$  and  $K^{*0}$ . Since baryons do not contain any constituent anti-quark, this indicates that leading baryons are likely to carry the initial quark and its quantum numbers. For mesons the quantitative interpretation of the data in terms of the static quark model suggested that fast kaons are likely to carry the primary quark and its quantum numbers and that leading kaons are produced predominantly in  $s\bar{s}$  events rather than in  $u\bar{u}$  and  $d\bar{d}$  events. No significant polarization transfer was observed for leading charged pions, though the quark model predicted for them the same polarization transfer as for kaons.

### 2.1. Measurement of the $\Lambda$ and $\Lambda_b$ longitudinal polarization

At the  $Z$  peak the Standard Model predicts for down-type quarks  $\langle P_L \rangle = -0.91$  for  $\sin^2 \theta_W = 0.232$ , including QCD corrections. The main question is whether and to which extent the primary quark polarization is transferred to the leading final state  $\Lambda(\Lambda_b)$

during the hadronization process. For the  $\Lambda_b$ , HQET predicts [15] the decoupling of the heavy quark degrees of freedom from the light quark ones [15]. Therefore, full polarization transfer is expected. For the  $\Lambda$ , one has to rely on the constituent model prediction, which is known to be violated in deep inelastic scattering (DIS), though at low  $x$  Bjorken.

The  $\Lambda$  longitudinal polarization was measured [16,17] using the fact that, in the parity violating decay  $\Lambda \rightarrow p\pi$ , S and P wave final states interfere giving rise to the asymmetric angular distribution  $W(\theta^*) \propto 1 + \alpha_\Lambda P_L \cos\theta^*$ , where  $\theta^*$  is the angle of the proton in the  $\Lambda$  rest frame, with respect to the polarization axis of the  $\Lambda$ . The value  $\alpha_\Lambda = 0.642 \pm 0.013$  is known from previous experiments [7]. Since  $\alpha_{\bar{\Lambda}} = -\alpha_\Lambda$ , by CP invariance, and  $\lambda(s) = -\lambda(\bar{s})$ , where  $\lambda(s)$  is the strange quark helicity,  $\Lambda$  and  $\bar{\Lambda}$  are expected to give, and it was indeed found in the data, the same slope. The comparison with theory was performed taking into account that the final selected sample contained also unpolarized  $\Lambda$ 's from the decay of other strange baryons ( $\Sigma, \Xi, \dots$ ),  $\Lambda$ 's produced during the fragmentation process,  $K_S^0$ 's and combinatorial background. The two experiments are consistent with the absence of depolarizing mechanisms. The result of one of them [16] is shown in figure 3.

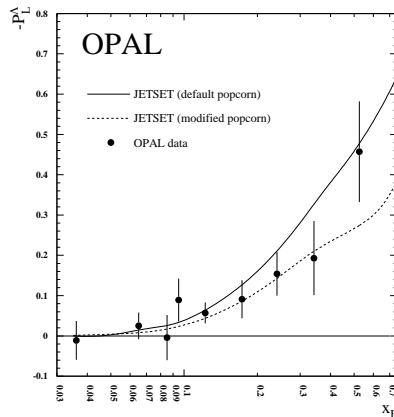


Fig. 3. Lambda longitudinal polarization as a function of  $x_E = 2E_\Lambda/\sqrt{s}$ , where  $E_\Lambda$  is the  $\Lambda$  energy in the laboratory system, compared to theoretical predictions.

The observation of a large polarization transfer will be exploited in polarized deep inelastic scattering experiments (see for instance [19]) to test the hypothesis of intrinsic proton strangeness [20] and then to shed light on the spin content of the proton.

The  $\Lambda_b$  longitudinal polarization was extracted from the measurement of lepton and neutrino energy spectra in the decays  $\Lambda_b \rightarrow \Lambda_c^+ l^- \bar{\nu}_l X$ ,  $\Lambda_c^+ \rightarrow \Lambda \pi^+ X$ . To model the  $\Lambda_b$  decay the HQET prediction was used: in the  $\Lambda_b$  rest frame, the lepton tends to be emitted anti-parallel and the anti-neutrino parallel to the  $\Lambda_b$  spin, giving, for the negatively polarized  $\Lambda_b$  in the lab frame, a harder lepton and a softer (anti-)neutrino spectra. The neutrino energy was obtained dividing the event in two hemispheres and subtracting the hemisphere visible energy to the beam energy. A recent average [21] gives  $-0.44_{-0.12}^{+0.14}$  and is consistent with the absence of depolarizing mechanisms, if a significant production of  $\Sigma_b, \Sigma_b^{(*)}$ , strongly decaying to  $\Lambda_b \pi$ , is taken into account.

## 2.2. Spin alignment of vector mesons

Information on particle production mechanisms can be obtained from measurements of the elements of the helicity density matrix  $\rho_{\lambda\lambda'}$ ,  $\lambda, \lambda' = 0, \pm 1$  for  $J^P = 1^-$  vector mesons. The diagonal elements of the matrix represent the probability that the particle has helicity  $\lambda$ .

In statistical models all helicity states of fragmentation quark pairs are equally likely to occur. Then, if the spin of primary quark is parallel to that of secondary antiquark, a transversely polarized ( $\lambda = \pm 1$ ) vector meson is produced; if it is anti-parallel, a pseudoscalar meson is produced with probability  $f$  and a longitudinally polarized ( $\lambda = 0$ ) vector meson with probability  $1 - f$ . In this model  $\rho_{00} = (1 - f)/(2 - f)$  and therefore  $0 < \rho_{00} < 0.5$ . In terms of ratio of pseudoscalar (P) to vector (V) meson production  $\rho_{00} = 1/2(1 - P/V)$ . A vector meson is said to be spin aligned if  $\rho_{00} \neq 1/3$ , i.e. if there is a non-uniform population of longitudinal and transverse states, regardless of the values of  $\rho_{1,1}$  and  $\rho_{-1,-1}$ . For heavy quark resonances, such as  $D^*$  and  $B^*$ , this model, together the HQET prediction of decoupling of the light quark degrees of freedom, predicts  $\rho_{00} = 1/3$ . A QCD-inspired model [22], describing the fragmentation process as the emission of soft gluons from the primary quark predicts  $\rho_{00} = 0$  while a model describing vector meson production  $V$  through the helicity conserving process  $q \rightarrow qV$  give [23]  $\rho_{00} = 1$ . Finally, in the most popular Lund string model and QCD cluster model, spin aspects of particle production are essentially ignored.

The element  $\rho_{00}$  was extracted from the measurement of the resonance production cross-section in different  $\theta^*$  intervals, where  $\theta^*$  is the angle of the meson decay product with respect to the meson polarization axis.

Two cases were studied:

a) vector meson  $\rightarrow$  two pseudo-scalars

The main experimental problems came from the presence of reflections from other resonances (both from imperfect particle identification and from other resonances decaying to the same particles) and from resonance shape distortions due to Bose-Einstein effect.

An isotropic distribution is expected for no spin alignment ( $\rho_{00} = \frac{1}{3}$ ) and proportional to  $\sin^2\theta^*$  for helicity  $\pm 1$  states and to  $\cos^2\theta^*$  for helicity 0 states.

Indication for spin alignment at high momentum fraction  $x_p$  was obtained at LEP [24,25,26,29]. The combined result of two experiments [24,29], for  $\phi \rightarrow KK$ ,  $x_p \geq 0.4$  is  $\rho_{00} = 0.49 \pm 0.05$  which is  $3.2\sigma$  from  $1/3$ . The combined result of two experiments [25,26] for  $K^{0*} \rightarrow K\pi$ , for  $x_p \geq 0.7$  is  $\rho_{00} = 0.54 \pm 0.06$  which is  $3.46\sigma$  from  $1/3$ . These results could be consistent with statistical models, though it would require a large suppression of pseudoscalar meson production in the hadronisation. They are in agreement with the model [23], which is however considered old-fashioned and is no more used in present high energy experiments.

Values consistent with  $1/3$  were found for  $\rho^0 \rightarrow \pi\pi$  and for  $D^{*\pm} \rightarrow D^0\pi \rightarrow K\pi\pi$  at all  $x_p$  (though some disagreement among experiments exists) and for  $\phi \rightarrow KK$  and  $K^{0*} \rightarrow K\pi$  at low  $x_p$ .

b) vector meson  $\rightarrow$  pseudo-scalar + vector

The decay  $B^* \rightarrow B\gamma$  was studied. An isotropic distribution is expected for no spin alignment and proportional to  $1 + \cos^2\theta^*$  for helicity  $\pm 1$  states and to  $\sin^2\theta^*$  for helicity 0 states.

The combined result of three experiments [27,28,29] is  $\rho_{00} = 0.33 \pm 0.04$  which, together with the measured  $V/(V + P) = 0.75 \pm 0.10$ , is consistent with a uniform population of spin states, as predicted by HQET.

Since all these resonances decay by strong or electromagnetic interactions, no separate measurement of  $\rho_{1,1}$  and  $\rho_{-1,-1}$  was possible.

### 2.3. Spin composition of $\Lambda$ baryon pairs

The measurement of the relative polarization of baryon-antibaryon pairs, selected with low  $Q^2$  in order to remove the baryons directly coming from the primary  $s\bar{s}$  pair, allowed to investigate the baryon production process. As an example, if the production of these pairs went through single gluon emission, in analogy to  $J/\Psi$ , the S=1 state would be expected to dominate. For  $\Lambda\bar{\Lambda}$  pairs the angular distributions are [30]  $dN/dy^* = 1 + \alpha_\Lambda^2 y^*$  for S=0 and  $dN/dy^* = 1 - \alpha_\Lambda^2/(3y^*)$  for S=1, where  $y^* = \cos\theta^*$  and  $\theta^*$  is the angle between the two hyperons' decay protons, each measured in its parent decay frame.

In the region  $Q = \sqrt{M_{\Lambda\bar{\Lambda}}^2 - 4m_\Lambda^2} < 2.5$  GeV, where a broad mass enhancement is observed,



it was found [31] that the fraction of the S=1 state contribution is  $0.71 \pm 0.07$ , consistent with a statistical spin distribution, indicating that  $\Lambda\bar{\Lambda}$  pair production goes through many QCD processes and baryon's decay.

### 3. Search for New Physics: the $\tau$ weak magnetic dipole moment

In the S.M. the weak magnetic dipole moment of the  $\tau$  lepton is zero at Born level. A calculation including higher order corrections gives [32,33]  $a_\tau^w = -(2.10 + i 0.61)10^{-6}$ . A measurement of  $a_\tau^w$  significantly different from this prediction would be an evidence for new physics beyond the Standard Model.

In analogy with the e.m. dipole moment, the weak one is introduced using the effective Lagrangian

$$\mathcal{L} = \frac{1}{2} \frac{ea_\tau^w}{2m_\tau} \bar{\psi} \sigma^{\mu\nu} \psi Z_{\mu\nu} \quad \text{and} \quad \mu_\tau^w = \frac{e}{2m_\tau} 2 \left( \frac{1 - 4\sin^2\theta_W}{4\sin\theta_W \cos\theta_W} + a_\tau^w \right) \quad (19)$$

with  $Z_{\mu\nu} = \partial_\mu Z_\nu - \partial_\nu Z_\mu$ . Keeping only up to linear terms in the spin and in the weak dipole moment and neglecting terms proportional to the electron mass, the tree level  $e^+ e^- \rightarrow \tau^+ \tau^-$  cross-section at the  $Z$ -peak can be written as the sum of a spin-independent term and a spin-dependent one, which is:

$$\frac{d\sigma^S}{d\Omega_{\tau^-}} \propto [ (s_{\tau^+}^{*x} + s_{\tau^-}^{*x})X_+ + (s_{\tau^+}^{*y} + s_{\tau^-}^{*y})Y_+ + (s_{\tau^+}^{*z} + s_{\tau^-}^{*z})Z_+ + (s_{\tau^+}^{*y} - s_{\tau^-}^{*y})Y_- ] \quad (20)$$

The presence of the dipole moment term in the Lagrangian induces therefore, in addition to the longitudinal ( $Z_+$ ) polarization term, single  $\tau$  transverse ( $X_+, Y_+$ ), P-odd, and normal ( $Y_-$ ), T-odd, polarization terms. Not including terms suppressed by the large value of  $\gamma = M_Z/2m_\tau$ , the transverse polarization terms are given by:

$$\begin{aligned} X_+ &= a_\tau \sin\theta_{\tau^-} - 2\gamma [4v_\tau^2 + (v_\tau^2 + a_\tau^2) \cos\theta_{\tau^-}] \text{Re}(a_\tau^w) \\ Y_+ &= -2v_\tau \gamma \beta \sin\theta_{\tau^-} [2a_\tau^2 + (v_\tau^2 + a_\tau^2) \cos\theta_{\tau^-}] \text{Im}(a_\tau^w) \end{aligned} \quad (21)$$

Introducing the  $\tau$  decay, for the spin-dependent term, with both  $\tau$ 's decaying semi-leptonically, it is obtained:

$$\frac{d\sigma^S}{d\cos\theta_{\tau^-} d\phi_{h\pm}} \propto [\alpha_h (\mp X_+ \cos\phi_{h\pm} + Y_\mp \sin\phi_{h\pm})] \quad (22)$$

where the reference frame is chosen such as  $\vec{p}_{\tau^-}$  is along z axis, the  $e^-$  beam direction in x-z plane,  $\theta_{\tau^-}$  is their relative angle and  $\phi_h$  is the azimuthal angle of the  $\tau^-$  decay product momentum in this frame.

Using a mixed up-down forward-backward angular asymmetry limits were set on the real and imaginary part of the weak dipole moment. To measure  $\phi_h$  one needs to reconstruct the  $\tau$  direction. This is possible with both  $\tau$ 's decaying semileptonically and leads to a two-fold ambiguity. It can be solved by measuring the vector  $\vec{d}_{min}$  of closest approach of the two  $\tau$  decay products with the help of a micro-vertex detector. In [34] for  $\pi - \pi$  events  $\epsilon = 60 - 80\%$ . The limits obtained at 95% C.L. were  $|\text{Re}(a_\tau^w)| < 4.5 \cdot 10^{-3}$  and  $|\text{Im}(a_\tau^w)| < 9.9 \cdot 10^{-3}$ .

### 4. Conclusions

In this paper I presented a number of examples of measurements related to spin performed during the last ten years at LEP and SLC. For lack of space, some important topics have been omitted, such as hard QCD studies, i.e. the measurement of the gluon spin, or the study of the  $W^+W^-Z/\gamma$  vertices.

As a perspective on the future, spin effects will be very useful tools for the search for physics beyond the Standard Model at a next higher energy linear collider. Among the most promising subjects, there is the study of spin observables in  $t\bar{t}$  events, sensitive to anomalous moments and

CP-violating form factors, and the use of polarized beams to reduce backgrounds from standard processes in the search for supersymmetric particles[35].

As an overall conclusion I would say that spin physics is clearly a central subject at  $e^+e^-$  colliders.

## 5. Acknowledgements

I would like to thank the organizers of the Workshop for the invitation. I would also like to thank A. Kotsinian, L. Serin, and D. Zerwas for their useful comments during the write-up of the paper.

## References

- [1] R. Alemany et al., *Nucl. Phys.* **B379** (1992) 3
- [2] J. Bernabeu et al., *Phys. Lett.* **B257** (1991) 219
- [3] ALEPH Collab., *Phys. Lett.* **B405** (1997) 191
- [4] M. Davier et al., *Phys. Lett.* **B306** (1993) 411
- [5] ALEPH Collab., Contribution to ICHEP98, Vancouver
- [6] P. Privitera, *Phys. Lett.* **B308** (1993) 163
- [7] Review of Particle Physics, *Europ. Phys. Jour.* **C3** (1998) 1
- [8] DELPHI Collab., *Phys. Lett.* **B404** (1997) 194
- [9] L3 Collab., *Phys. Lett.* **B377** (1996) 313
- [10] ALEPH Collab., *Phys. Lett.* **B346** (1995) 379
- [11] OPAL Collab., *Z. Phys.* **C75** (1997) 593
- [12] SLD Collab., *Phys. Rev. Lett.* **78** (1997) 4691
- [13] D. Karlen, Plenary talk at ICHEP98, Vancouver
- [14] SLD Collab., *Phys. Rev. Lett.* **78** (1997) 3442 Erratum-ibid. **79** (1997) 959
- [15] T. Mannel et al., *Phys. Lett.* **B255** (1991) 593; J. G. Korner and M. Kramer, *Phys. Lett.* **B275** (1992) 495; A. Falk and M. E. Peskin, *Phys. Rev.* **D49** (1994) 3320; T. Mannel and G. Schuler, *Phys. Lett.* **B279** (1992) 194
- [16] OPAL Collab., *Europ. Phys. Jour.* **C2** (1998) 49
- [17] ALEPH Collab., *Phys. Lett.* **B374** (1996) 319
- [18] ALEPH Collab., *Phys. Lett.* **B365** (1996) 437
- [19] The Compass Collab., Proposal, CERN/SPSLC 96-14  
Addendum 1, CERN/SPSLC 96-30.
- [20] J. Ellis et al., *Phys. Lett.* **B353** (1995) 319
- [21] R. Van Kooten, Talk given at ICHEP98, Vancouver
- [22] J. E. Augustin and F. M. Renard, *Nucl. Phys.* **B162** (1980) 341
- [23] J. F. Donoghue, *Phys. Rev.* **D19** (1979) 2806
- [24] DELPHI Collab., *Phys. Lett.* **B406** (1997) 271
- [25] DELPHI Collab., *Z. Phys.* **C73** (1996) 61
- [26] OPAL Collab., *Phys. Lett.* **B412** (1997) 210
- [27] ALEPH Collab., *Z. Phys.* **C69** (1996) 393
- [28] DELPHI Collab., *Z. Phys.* **C68** (1995) 353
- [29] OPAL Collab., *Z. Phys.* **C74** (1997) 437
- [30] G. Alexander and H. J. Lipkin, *Phys. Lett.* **B352**(1995) 162
- [31] OPAL Collab., *Phys. Lett.* **B384** (1996) 377
- [32] J. Bernabeu et al., *Nucl. Phys.* **B436** (1995) 474

- [33] J. Bernabeu et al., *Phys. Lett.* **B326** (1994) 168
- [34] L3 Collab., *Phys. Lett.* **B426** (1998) 207
- [35] H. E. Haber, Proceedings of the 21st SLAC Summer Institute on Particle Physics: Spin Structure in High Energy Processes, SLAC, Stanford, CA, 26 July 1993